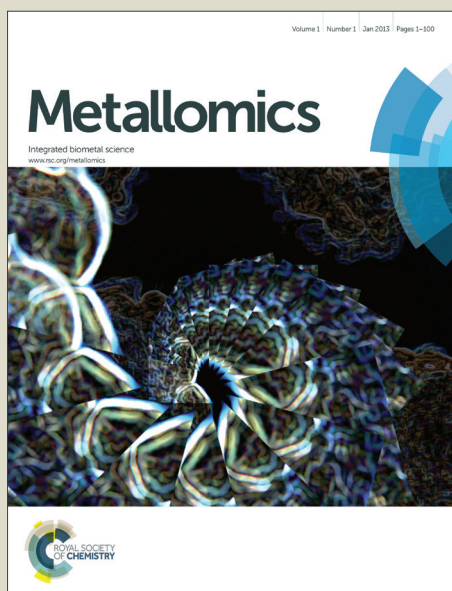


Metallomics

Accepted Manuscript



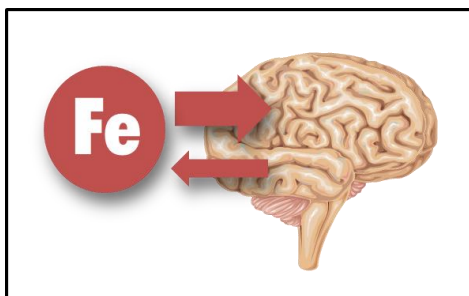
This is an *Accepted Manuscript*, which has been through the Royal Society of Chemistry peer review process and has been accepted for publication.

Accepted Manuscripts are published online shortly after acceptance, before technical editing, formatting and proof reading. Using this free service, authors can make their results available to the community, in citable form, before we publish the edited article. We will replace this *Accepted Manuscript* with the edited and formatted *Advance Article* as soon as it is available.

You can find more information about *Accepted Manuscripts* in the [Information for Authors](#).

Please note that technical editing may introduce minor changes to the text and/or graphics, which may alter content. The journal's standard [Terms & Conditions](#) and the [Ethical guidelines](#) still apply. In no event shall the Royal Society of Chemistry be held responsible for any errors or omissions in this *Accepted Manuscript* or any consequences arising from the use of any information it contains.

1
2
3
4
5
6
7
8
9
10
11
12
13
14
15
16
17
18
19
20
21
22
23
24
25
26
27
28
29
30
31
32
33
34
35
36
37
38
39
40
41
42
43
44
45
46
47
48
49
50
51
52
53
54
55
56
57
58
59
60



**A novel approach for studying brain iron homeostasis
in animal models using stable isotope tracers**

ARTICLE

Imbalance of iron influx and efflux causes brain iron accumulation over time in the healthy adult rat

Cite this: DOI: 10.1039/x0xx00000x

Jie-Hua Chen,^{a, b} Nadia Singh,^a Huimin Tay^a and Thomas Walczyk*^{a, c}

Received 00th January 2012,

Accepted 00th January 2012

DOI: 10.1039/x0xx00000x

www.rsc.org/

Brain iron accumulation is supposed to play a central role in neurodegeneration by inducing oxidative stress. Currently it is unknown to which extent iron entering brain over lifetime exchanges with body iron or if uptake of iron is unidirectional without significant efflux from brain. To study brain iron dynamics *in vivo*, up to three stable isotope tracers were fed continuously with a standard rodent diet up to 5 months to healthy adult male Wistar rats (n=8) in a staggered design. Brain iron uptake was found to be bi-directional but iron influx and efflux were unbalanced leading inevitably to brain iron accumulation over time. Brain iron turnover was found to be very low at a half-life of ca. 9 months for tracer iron entering brain. Observed tracer accumulation in brain iron can be extrapolated to an increase of brain iron by ca. 30% in the healthy rat from early adulthood to the end of their lives. In contrast to current beliefs that brain uptake of dietary iron is negligible during adulthood following short-term radiotracer studies, our long-term feeding experiments point to a possible role of diet in brain iron accumulation and, subsequently, neurodegeneration.

Introduction

Iron is the most abundant trace element in brain. The ease in donating and accepting electrons renders iron an indispensable cofactor for a plethora of enzymatic reactions involved in neurogenesis, brain development and cognition sustenance¹. However, iron is potentially toxic if not bound to iron binding proteins such as transferrin, ferritin or iron containing enzymes. Unbound iron can induce oxidative stress via catalyzing the formation of ROS, i.e. highly reactive oxygen species^{2,3}.

Age-related brain iron deposition has been observed in all species examined, including mice, rats, monkeys and humans⁴⁻⁹. Progressively elevated brain iron with age may pose a threat to the brain's oxygen-rich environment by inducing ROS formation¹⁰⁻¹². Many lines of evidence support now the hypothesis that brain iron accumulation with age might be implicated in the pathogenesis of age-related neurodegeneration with iron induced oxidative stress as the underlying mechanism^{13,14}. It has been speculated that iron deposition in brain could be reflective of dietary iron exposure and an overall accumulation of iron in the body.

In an earlier study we have pioneered the use of stable iron isotopes for tracing brain iron uptake from diet in adult rats¹⁵. In agreement with earlier radiotracer studies¹⁶⁻¹⁸ we found that absolute brain iron uptake was very low (< 0.001% of dietary iron). At the same time we could show that this small amount constituted about 9% of total brain after four months of tracer/iron feeding. This observation became only possible by using stable isotope tracers which can be fed continuously in

contrast to radiotracers which were commonly given once by injection in earlier studies. The key question that remains now is whether iron is imported in brain without export or if more iron is imported than exported from brain and at which rate. The first scenario would not affect brain iron content in the long-term and tracer influx would reflect brain iron turnover. The second scenario would point to gradual accumulation of iron over time.

In our first study we fed a single tracer continuously to mimic dietary iron influx into brain. In the present study, we fed up to three stable isotope tracers to rats in a staggered design to assess iron influx/efflux and the half-life of dietary iron in brain. As in our first study, we conducted experiments in adult rats since the rate of whole brain iron accumulation slows down after the first three decades of life⁴ and it is possibly the amount of iron accumulated after that contributes mainly to the development of the disease.

Experimental section

Study Design

The fate of dietary iron was investigated by feeding up to three different stable isotope tracers (⁵⁴Fe, ⁵⁷Fe and ⁵⁸Fe) with the diet. While the dual-isotope feeding scheme provides a qualitative assessment of brain iron balance, the triple-isotope feeding scheme permits to study iron dynamics quantitatively by comparing rates of iron influx and iron efflux and by

estimation of the half-life of iron taken up by the brain, respectively.

The dual isotope feeding scheme involves the staggered administration of two different stable iron isotopes, Tracer 1 (T_1 ; ^{57}Fe) and Tracer 2 (T_2 ; ^{54}Fe) which are fed continuously over an equal duration of time. Two possible scenarios are illustrated in Fig. 1. If there is no export of iron after its

deposition into brain, tracer amount ratios in brain must equal that of the feed at the time of sacrifice (see Fig. 1a). The more of imported iron is exported from brain, the larger is the difference in the amount ratio of both tracers in brain and feed at the end of the study (see Fig. 1b).

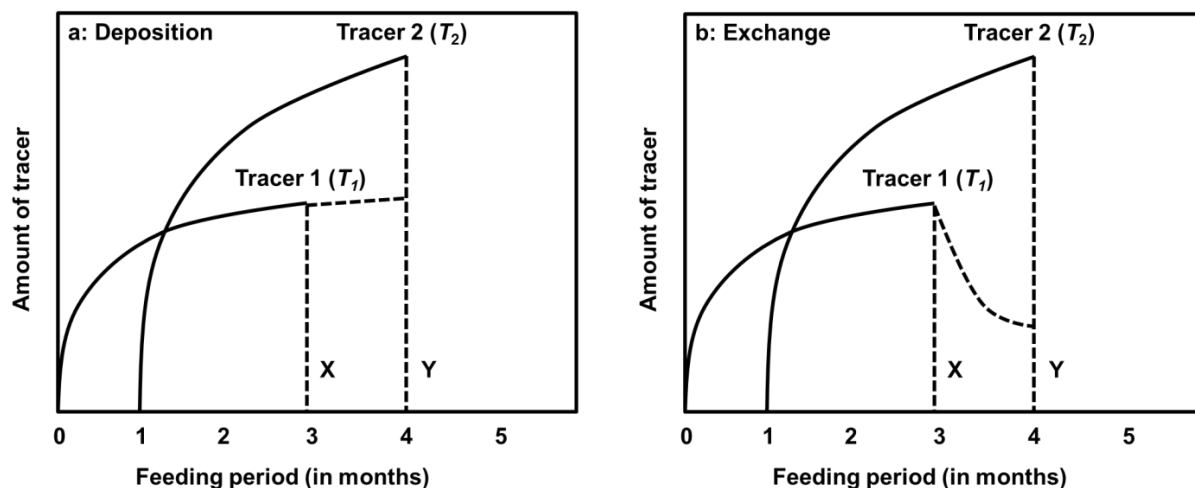


Fig. 1 Dual-isotope tracing for studying iron import and export from organs/tissues. Tracer 1 (T_1) is administered from month 1 to 3 and Tracer 2 (T_2) from month 2 to 4 together with the feed. Vertical lines X and Y indicate the time points when tracer administration is terminated. Dashed curve lines represent the fate of the tracer thereafter. In Fig. 1a, iron is deposited in the brain in a uni-directional manner, resulting in the accumulation of both tracers in the brain over time. Without iron export from brain, the amount ratio of both tracers in brain should be equal to the amount ratio in the consumed feed. In Fig. 1b, iron enters the brain in a bi-directional manner. If iron is exported from brain, the amount of the first tracer in brain will decrease when tracer administration is terminated. The amount ratio of both tracers in the brain is then lower than the ratio in the consumed feed.

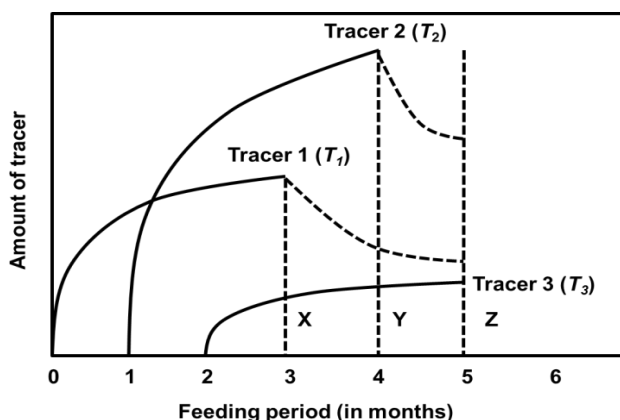


Fig. 2 Triple-isotope tracing for modeling kinetics of iron release from organs/tissues. The first tracer (T_1) is administered from month 1 to 3, the second tracer (T_2) from month 2 to 4 and the third tracer (T_3) from month 3 to 5. Vertical lines X and Y indicate time points when tracer administration is terminated. Dashed curve lines represent the fate of the tracer thereafter. At the time of sacrifice (Z), amount ratios of tracers in brain differ from that of the feed when tracer has been exported from brain. Differences in amount ratios T_1/T_3 and T_2/T_3 in brain will be proportional to the rate by which deposited iron tracer is released from brain.

The triple-isotope feeding scheme involves the staggered administration of three different iron isotopes, Tracer 1 (T_1 ; ^{57}Fe), Tracer 2 (T_2 ; ^{54}Fe) and Tracer 3 (T_3 ; ^{58}Fe), respectively, see Fig. 2. If iron taken up from diet is exported from brain, tracer amount ratios in brain should be lower than that of the feed. For iron export, the amount ratio of T_1 to T_3 in the brain

relative to that in the diet should be lower than that of T_2 to T_3 , since T_1 is administered first, followed by T_2 and lastly T_3 . Differences in amount ratios between tracers, i.e. $n(T_1)/n(T_3)$ and $n(T_2)/n(T_3)$ can be used to model kinetics of iron release from brain.

Animals

Eight male Wistar rats (6 to 8-month old, body weight 625 ± 48 g) were obtained from a local supplier (Laboratory Animals Centre, LAC) and housed individually at a temperature of 21 ± 1 °C, with a humidity of 55 ± 5 % and a 12 hour light/dark cycle. Rats were randomly assigned to the two different feeding groups, *DI* (dual-isotope feeding scheme) group ($n=3$) and *TI* (triple-isotope feeding scheme) group ($n=5$). The body weight of the rats and the amount of water consumed by the rats were monitored weekly. All experimental protocols were reviewed and approved by Institutional Animal Care and Use Committee (IACUC) of National University of Singapore (NUS).

All rats had *ad libitum* access to a standard rat chow diet (Teklad 2018S Rodent Diet, Harlan, Indianapolis, USA; iron concentration 200 mg/kg) and isotopically enriched drinking water during the course of the study. In the *DI* group, the feeding period lasted for 4 months. The first tracer T_1 (^{57}Fe) was fed during month 1-3 while the second tracer T_2 (^{54}Fe) was fed during month 2-4 via the drinking water (see Fig. 1). The average concentrations of ^{54}Fe and ^{57}Fe in the drinking water for the *DI* group was 11.215 ± 0.021 and 5.207 ± 0.045 $\mu\text{g/g}$ respectively. In the *TI* group, the feeding period was extended to 5 months to allow for feeding of an additional enriched

1 stable iron isotope. As for the *TI* group, all tracers were
2 administered via drinking water. The first tracer T_1 (^{57}Fe) was
3 fed during months 1 to 3, the second tracer T_2 (^{54}Fe) during
4 month 2-4 and the third tracer T_3 (^{58}Fe) from month 3 to 5,
5 respectively (see Fig. 2). The average concentrations of ^{54}Fe ,
6 ^{57}Fe and ^{58}Fe in the drinking water for *TI* group were, $11.201 \pm$
7 0.025 , 5.216 ± 0.030 and 3.004 ± 0.016 $\mu\text{g/g}$, respectively.

8 In order to maintain dietary iron supply in both groups
9 constant over the course of the study, differences in iron intake
10 induced by differences in tracer concentration in the drinking
11 water were balanced by adding iron of natural isotopic
12 composition to the water. As in our previous study, the pH of
13 the drinking water was maintained at 2.5 in order to ensure no
14 precipitation of iron. Water acidity should not affect water
15 consumption as rats do not have any taste receptors for water¹⁹.
16 Isotopic enriched water was changed every 3-4 days. The
17 masses of the drinking bottles before and after each change of
18 water supply were recorded in order to accurately assess dietary
19 iron tracer intake over the course of the study.

20 Stable isotope labels

21 All isotopic labels were prepared from iron metal
22 (Chemgas, France), isotopically enriched in ^{54}Fe (99.873 \pm
23 0.010 % ^{54}Fe), ^{57}Fe (95.910 \pm 0.011 % ^{57}Fe) and ^{58}Fe (99.9109
24 \pm 0.0013 % ^{58}Fe). Isotopically enriched iron spikes were
25 dissolved in 37% HCl and diluted with water to yield 5 M HCl
26 solutions. Iron concentrations were determined against a
27 commercially available standard (Titrisol[®]; FeCl_3 in 15% HCl,
28 1000 mg Fe; Merck). Negative thermal ionization mass
29 spectrometry (NTI-MS) was used to determine the isotopic
30 composition of the spike solutions using the method developed
31 by²⁰ with modifications. The concentrations of iron in the spike
32 solutions were determined by reversed isotope dilution mass
33 spectrometry against the prepared iron standard.

34 All sample preparation work was performed in a class
35 10,000 clean room equipped with class 10 fume hoods. Only
36 teflon labware or disposable plastic labware was used. Plastic
37 lab ware was pre-cleaned by soaking in 10% (v/v) HNO_3
38 (Merck, USA) for 12 hrs and teflon labware by boiling in half-
39 concentrated HNO_3 . Acids and reagents used were of
40 analytical-reagent grade. Acids were purified further by sub-
41 boiling distillation before use. Water used throughout the study
42 was ultrapure 18.2 Ω Milli-Q[®] water (Millipore, Billerica,
43 Massachusetts, USA).

44 Blood and tissue sampling

45 Blood samples were collected monthly for the
46 determination of hemoglobin concentration and to assess
47 changes in iron isotopic compositions in the rat blood
48 throughout the feeding period. During the study, blood was
49 collected from the tail artery of the rats using 23G needles
50 under light isoflurane anesthesia (Webster Veterinary Patterson
51
52
53
54
55
56
57
58
59
60

Company, USA). At the end of the study, blood samples were
obtained via cardiac puncture. Blood samples were collected in
EDTA coated vacutainers and stored at -20 $^\circ\text{C}$ before
elemental and isotopic analysis.

Tissue sampling followed the procedure as described for our
earlier study¹⁵. In brief, animals were sacrificed by hyper-
perfusion, i.e. effective removal of blood from tissues by
washing of vessels and organs *in situ* with excessive volumes of
Ringer's solution (NaCl 0.85%, KCl 0.025%, CaCl_2 0.03%,
 NaHCO_3 0.02%). Heparin (5 I.U. heparin/mL) was added to the
solution to prevent blood clotting during the perfusion process.
Organs such as heart, kidneys, liver, muscle and brain were
harvested and stored at -20°C prior to isotopic analysis.

Iron elemental and isotopic analysis

The collected samples were freeze dried and grinded into
fine powders. For *DI* group samples, a weighed aliquot of the
homogenized tissue was transferred into a teflon vessel together
with a known amount of enriched ^{58}Fe label to determine the
amount of natural iron in the sample following isotope dilution
principles (see Data analysis). The mixture was mineralized in a
microwave digestion system (Ethos 1, Milestone, Sorisole,
Italy). Tissues collected from the *TI* group were digested
directly without addition of an additional tracer for iron
quantification. After mineralization, iron in the solution was
separated by ion-exchange chromatography using a strongly
basic ion-exchange resin (Dowex AG 1-X8; 200 - 400 mesh,
Sigma, St. Louis, USA). The eluate obtained was alkalinized by
addition of 25% ammonium hydroxide (Merck, Darmstadt,
Germany) for precipitating sample iron as ferrihydrite. The iron
precipitate was stored dry until isotope ratio analysis. The iron
isotopic composition of the isotopic labels and the prepared
samples were determined by negative thermal ionization mass
spectrometry (NTI-MS) using FeF_4^- molecular ions and a
rhenium double-filament ion source with details described
earlier²⁰. Further technical details are described in an earlier
publication¹⁵.

Concentration of haemoglobin in the rat blood sample was
indirectly determined in triplicate through iron concentration in
the blood¹⁵. Iron content of blood samples was analyzed by
graphite furnace atomic absorption spectrometry (GF-AAS)
(Varian AA240 Zeeman/GTA120, Varian Inc., Palo Alto, CA,
USA) by external calibration with an iron standard solution.

Data analysis

The amount ratio of tracers in the brain described were
determined following established procedures for isotope
dilution analysis using Eqn. (1)^{20,21} and the abundance of the
different isotopes in each enriched isotopic label a and the
measured isotope ratios in the sample R .

$$\begin{bmatrix}
 {}^{54}a_{nat} & {}^{54}a_{iso,54} & {}^{54}a_{iso,57} & {}^{54}a_{iso,58} \\
 {}^{57}a_{nat} & {}^{57}a_{iso,54} & {}^{57}a_{iso,57} & {}^{57}a_{iso,58} \\
 {}^{58}a_{nat} & {}^{58}a_{iso,54} & {}^{58}a_{iso,57} & {}^{58}a_{iso,58} \\
 {}^{56}a_{nat} & {}^{56}a_{iso,54} & {}^{56}a_{iso,56} & {}^{56}a_{iso,56}
 \end{bmatrix}
 \begin{bmatrix}
 \frac{n({}^{nat}Fe)}{n({}^{tot}Fe)} \\
 \frac{n({}^{54}Fe)}{n({}^{tot}Fe)} \\
 \frac{n({}^{57}Fe)}{n({}^{tot}Fe)} \\
 \frac{n({}^{58}Fe)}{n({}^{tot}Fe)}
 \end{bmatrix}
 =
 \begin{bmatrix}
 \frac{{}^{54/56}R_{sample}}{1 + \sum^i R_{sample}} \\
 \frac{{}^{57/56}R_{sample}}{1 + \sum^i R_{sample}} \\
 \frac{{}^{58/56}R_{sample}}{1 + \sum^i R_{sample}} \\
 \frac{{}^{56/56}R_{sample}}{1 + \sum^i R_{sample}}
 \end{bmatrix}
 \quad (1)$$

In a sample spiked with three iron isotopic labels (enriched ${}^{54}\text{Fe}$, ${}^{57}\text{Fe}$ and ${}^{58}\text{Fe}$), the amount of each of iron isotopes ${}^{54}n$, ${}^{57}n$, ${}^{58}n$ and ${}^{56}n$ is determined by the isotopic abundances a and the amounts (in moles) of each of the tracers in the blend ($n({}^{nat}\text{Fe})$, $n({}^{54}\text{Fe})$, $n({}^{57}\text{Fe})$ and $n({}^{58}\text{Fe})$). The iron isotopic abundance ${}^W a$ ($W=54, 56, 57$ and 58) for both isotopically enriched tracers ($iso,54$; $iso,57$; $iso,58$) and natural iron (nat) can be obtained from the sum of all measured isotope abundance ratios $\sum^i R$ with ${}^{56}a$ as the common denominator. The molar amount of the tracers is related to the measured isotope ratios R_{sample} via the total amount of iron in the sample $n({}^{tot}\text{Fe})$ and the abundance ${}^W a$ of the isotope in natural iron and the tracers. In sum, the abovementioned relationship can be expressed in a matrix form which can be solved to deliver the molar ratio of a given spike relative to natural iron in the sample.

Efflux Rate Index Based on Eqn. (1), the amount ratio of two tracers in a tissue sample with the amount of the last administered tracer as the common denominator, e.g. $n({}^{57}\text{Fe})/n({}^{54}\text{Fe})$, can be calculated from the molar ratio of the tracers [$n({}^{nat}\text{Fe})$, $n({}^{54}\text{Fe})$, $n({}^{57}\text{Fe})$ and $n({}^{58}\text{Fe})$] relative to the total amount of iron in the sample [$n({}^{tot}\text{Fe})$]. The calculated amount ratio of tracers in the brain relative to that in the diet was designated as the Efflux Rate Index. The higher the Efflux Rate Index, the less of the tracer taken up by brain was transported out of the brain after termination of tracer administration and the lower is the efflux rate.

Tissue iron uptake (DI group) Based on Eqn. (1), the amount of total iron $n({}^{tot}\text{Fe})$ in the sample aliquot in the DI group was calculated from the $n({}^{58}\text{Fe})/n({}^{tot}\text{Fe})$ ratio and the known amount of added ${}^{58}\text{Fe}$ spike (in moles) before digestion. The total amount of ${}^{57}\text{Fe}$ tracer in the sample could then be calculated from the $n({}^{57}\text{Fe})/n({}^{tot}\text{Fe})$ ratio and $n({}^{tot}\text{Fe})$ in the analyzed sample. Total amount of ${}^{54}\text{Fe}$ tracer in the sample could be calculated in the same way as that for the ${}^{57}\text{Fe}$ tracer. Total amount of tracer in the organ was calculated by taking the mass of tissue analyzed and the total mass of the organ/sample into account. Absolute tissue iron uptake (% of iron fed) was calculated as total moles of tracer recovered in the tissue relative to total moles of tracer consumed.

The amount of iron transferred into each tissue is expressed relative to the amount of total iron in the analyzed tissue as relative tissue iron uptake (% of tissue iron coming from feed). For the TI group, all available enriched stable iron isotope

tracers had already been used during the feeding and were not available any more to quantify tissue iron following isotope dilution principles. Iron concentrations were therefore determined by graphite furnace absorption spectrometry and using standard addition techniques.

Evaluation of kinetics of iron efflux (TI group) A single compartment model was used to estimate tracer efflux rates for each individual organ in the TI group. The amount of the last administered tracer (T_3 ; ${}^{58}\text{Fe}$) in the organ at sacrifice was set to 100% (Efflux Rate Index of 1.0). Efflux rate indices for the first administered tracer (T_1 ; ${}^{57}\text{Fe}$) and the second administered tracer (T_2 ; ${}^{54}\text{Fe}$) were expressed relative to the efflux rate index of tracer T_3 and plotted against the time period between termination of tracer administration and sacrifice. The obtained data points were fitted by the Windows version of the SAAM/Consaam software, WinSAAM (Simulation, Analysis and Modelling) to determine tracer efflux rates of iron from the respective organ.

Statistical analysis

Comparisons of absolute/relative tissue iron uptake and iron efflux between different tissues were conducted by performing an independent sample t -test for equality of means using SPSS version 20 software (SPSS Inc., Chicago, USA). In all tests, a value of $P \leq 0.05$ was considered statistically significant.

Results and discussion

Results

No premature deaths were observed among the treated rats. The total amount of consumed feed, water and iron isotopes of each feeding group is summarized in Table 1. The rats showed a moderate increase in body weight in both groups over the course of the study from 643 ± 43 g at the beginning to 692 ± 49 g at the end in for the DI group and from 613 ± 49 g to 713 ± 61 g for the TI group which is consistent with adult aging. The blood hemoglobin concentrations of each rat were within the reported normal range of 130 – 170 g Hb/L²² at the beginning (161 ± 13 g Hb/L) and end of the studies (159 ± 12 g Hb/L) for the DI group and 148 ± 8 g Hb/L and 149 ± 8 g Hb/L for the TI group, with minor variations within each study.

Table 1 Total amount of consumed feed, water and iron tracers for the *DI* group (4 month of feeding) and the *TI* group (5 month of feeding)

Group	Consumed feed [kg]	Consumed water [L]	Consumed natural iron [mmol]	Consumed iron tracers from water		
				Tracer ^{57}Fe [mmol]	Tracer ^{54}Fe [mmol]	Tracer ^{58}Fe [mmol]
<i>DI</i>	2.93 ± 0.15	2.57 ± 0.20	10.49 ± 0.54	0.350 ± 0.030	0.800 ± 0.080	-
<i>TI</i>	3.80 ± 0.20	3.56 ± 0.54	13.61 ± 0.70	0.400 ± 0.060	0.89 ± 0.13	0.220 ± 0.033

Tracer analysis of blood samples The measured amount ratio of tracer to total iron in blood carries information about the bioavailability of tracer iron. For comparison of data obtained for different tracers, amount ratios of tracer to total iron were adjusted for dose to that of the ^{57}Fe tracer for each individual rat using the tracer concentration ratios in the drinking water for normalization. After dose adjustment, the amount ratios of tracer to total blood iron

were comparable for the different iron tracers in blood ($p=0.91$ for ^{54}Fe tracer in *DI* group; $p=0.33$ for ^{54}Fe tracer and $p=0.08$ for ^{58}Fe tracer in *TI* group; see Fig. 3 and 4). As can be expected, amount ratios of tracer to total iron increased steadily over time until termination of tracer feeding on from which the ratios declined due to blood iron turnover. A trend towards a slower increase in amount ratios of tracer to total iron over time was observed.

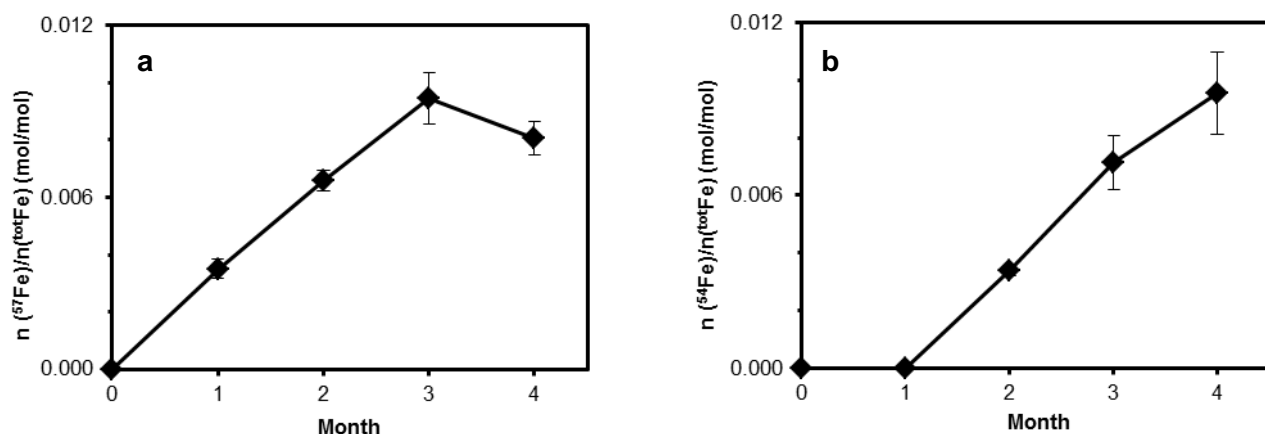
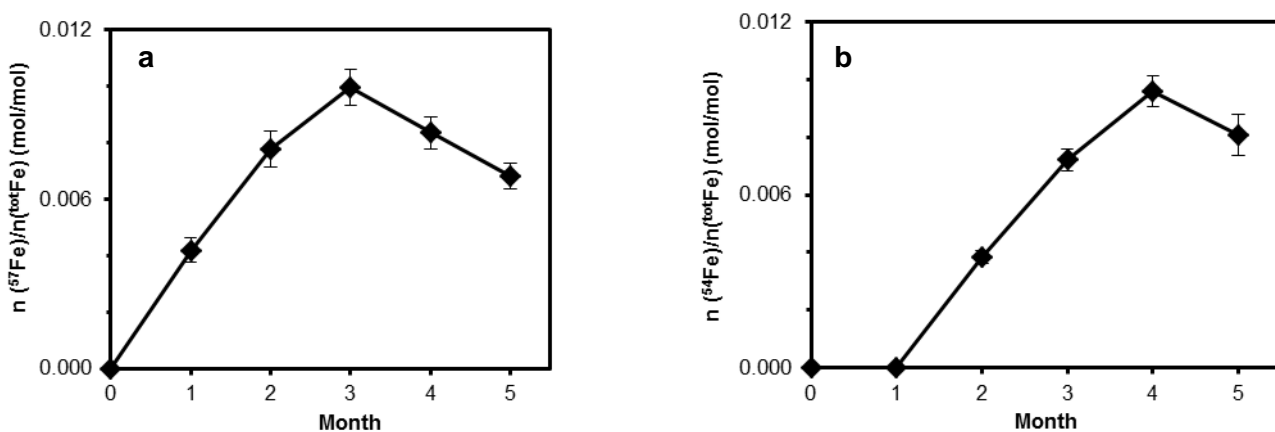


Fig. 3 Amount ratios of tracer (Fig. 3a: ^{57}Fe tracer; Fig. 3b: ^{54}Fe tracer) to total iron (mol/mol) in blood against time for the *DI* group (n = 3 rats). Feeding of the ^{57}Fe tracer was terminated at the end of month 3. Amount ratios were adjusted to differences in tracer concentration in the diet



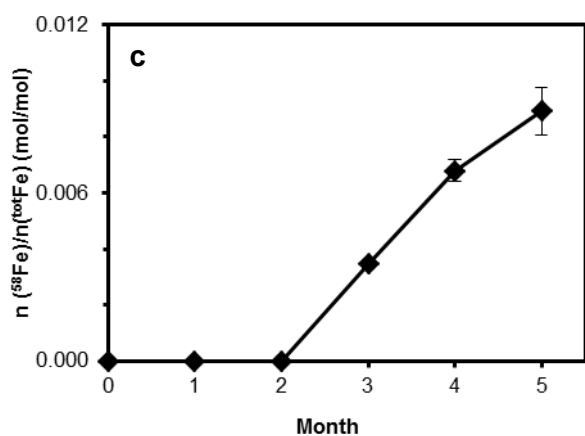


Fig. 4 Amount ratios of tracer (Fig. 4a: ^{57}Fe tracer; Fig. 4b: ^{54}Fe tracer; Fig. 4c: ^{58}Fe tracer) to total iron (mol/mol) in blood against time for the *TI* group ($n=5$ rats). Feeding of the ^{57}Fe tracer was terminated at the end of month 3 and that of the ^{54}Fe tracer at the end of month 4. Amount ratios were adjusted to differences in tracer concentration in the feed.

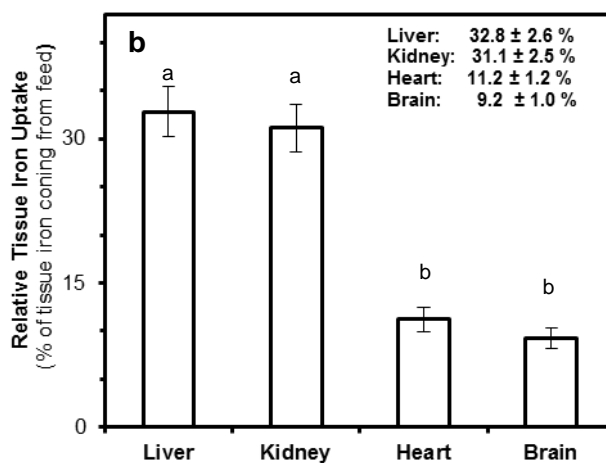
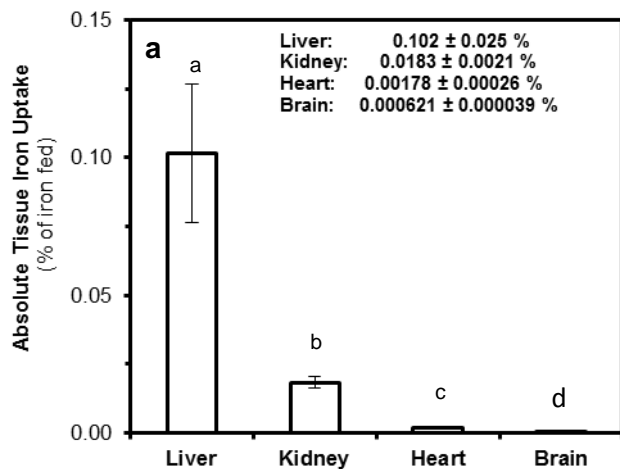


Fig. 5 Tissue iron uptake. Fig. 5a shows the percentage of dietary iron recovered in rat brains of the *DI* group ($n=3$ rats). Recoveries were calculated as the amount of ^{54}Fe tracer recovered in the organ relative to total amount of ^{54}Fe tracer given (in %). Fig. 5b shows the percentage of tissue iron in rat organs of the *DI* group coming from feed. Relative tissue iron uptake was calculated as the amount of ^{54}Fe tracer recovered in the organ coming from feed relative to the total amount of iron in the organ (in %). Different lower case letters indicate statistical significant differences between tissues ($p \leq 0.05$). Values are given as arithmetic means \pm SD ($n=3$)

Iron turnover in tissue - Qualitative assessment (*DI* group)

Muscle tissues exhibited tracer amount ratios that were the closest to that of the diet, demonstrating the lowest iron turnover rate among all analyzed tissues. After normalization of Efflux Rate Indices to muscle tissue, blood exhibited the highest turnover rate among major body iron pools (see Fig. 6). Efflux Rate Indices were all lower than 1.0 which indicates that more iron was replaced in the studied organs over the observational period than in muscle tissue as the iron pool showing the slowest iron turnover. The Efflux Rate Index of brain of 0.93, was higher than that of the other tissues, showing that iron was exported from brain at a slower rate as compared to other organs. The Efflux Rate Index of brain exhibited no difference with that of heart ($p=0.18$) whereas the Efflux Rate Index of liver showed no significant difference to those of kidney ($p=0.46$) and blood ($p=0.23$) but was significantly lower than that of heart ($p=0.01$) and brain ($p=0.001$), respectively.

Tissue iron uptake for the *DI* group Fig. 5 shows the absolute and relative iron uptake by different tissues in the *DI* group. Absolute iron uptake by different tissues was significantly different from each other and ranged from 0.00062% in brain to 0.102 % in liver in the present study (see Fig. 5a). Fig. 5b shows the percentage of tissue iron in rat organs of the *DI* group coming from feed (relative tissue iron uptake). Relative iron uptake of the analyzed tissues was of the same order of magnitude (9.2% - 32.8%) despite the marked differences in absolute iron uptake (0.000621% - 0.102% of the tracer dose). Relative iron uptake of brain was comparable to that of heart ($p=0.10$) and that of liver was comparable to that of the kidneys ($p=0.46$) while relative iron uptake of both brain and heart was significantly different from liver and kidneys ($p=0.001$).

Iron turnover in tissue - Quantitative assessment (*TI* group)

For the triple-isotope feeding scheme, iron turnover of different tissues was quantitatively evaluated by plotting the normalized Efflux Rate Index against time difference between terminations of tracer feeding and sacrifice (see Fig. 7). Dietary iron was found to be released from liver, kidney, heart, brain and blood at different efflux rate. Efflux rates expressed as % of tracer in brain released per month and tracer half-lives in the studied tissues was calculated using a single compartment model (see Table 2). Consistent with findings for the *DI* group, brain iron exhibited the lowest efflux rate (8.2 ± 3.1 % of tracer per month) among the measured tissues in the *TI* group. The half-life of dietary iron taken up by the brain was estimated to be 9.4 ± 3.2 months, the longest half-life among all analyzed tissues.

Table 2 Efflux rates and half-lives of dietary iron in the rat tissues in *TI* group*

	Liver	Kidney	Heart	Brain	Blood
Efflux rate (% tracer / month)	20.5 ± 6.6 ^a	19.8 ± 6.8 ^a	11.5 ± 2.1 ^b	8.2 ± 3.1	37.6 ± 9.6 ^a
Half-life of dietary iron (month)	3.7 ± 1.3 ^a	4.2 ± 1.9 ^a	6.2 ± 1.2 ^b	9.4 ± 3.2	2.0 ± 0.6 ^a

* The values of efflux rate and half-life of dietary iron in different tissues were compared with those in brain. Lower case indicates statistical difference ($p \leq 0.05$) whereas lower case b means no statistical difference

Discussion

In the present study we confirmed the major finding of our previous study¹⁵. The marginal amount of brain iron taken up from diet (0.00062%) after 4 months of feeding constituted ca. 9% of brain iron at sacrifice. While this does not challenge the finding from earlier radioisotope experiments that the absolute amount of iron uptake by brain is very low, it points to brain iron homeostasis and dietary iron intake as key factors in brain iron accumulation in ageing and possibly in neurodegeneration.

Our studies differ in many ways from earlier radiotracer studies due to the different scope of our experiments. Research interests in the past lied mostly in the developmental stage with limited focus on the effect of dietary iron on brain iron balance^{17, 23-27}. Because brain iron uptake is age-dependent^{28, 29} and dietary iron taken up by brain and its later release is a long-term process, it was imperative for us to study brain iron dynamics by feeding tracer continuously to adult and not to weaning/young rats. Our studies were conducted in 6-8 months old rats, corresponding to twenty-odd human years. The postmortem study by Hallgren and Sourander (1958)⁴ demonstrated that the rate of brain iron accumulation increases steeply during the first two decades, slows down in the third decade, and reaches a "plateau" or may increase very slowly thereafter. The change in brain iron accumulation rate suggests a change in brain iron dynamics including iron import/export over the course of life. As relatively large amounts of iron are required early in life for brain development, it is possible that the amount of iron accumulating during adulthood when brain

development can be considered complete, contributes to the development of iron-related neurodegenerative diseases. Similar to humans, iron was found to increase steeply in rat brain early in life but slows down at about the fourth month of life^{23, 30-33}.

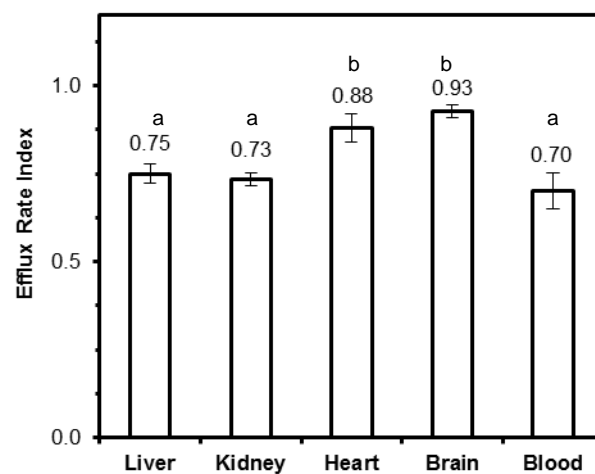


Fig. 6 Efflux Rate Index of different tissues for the *DI* group (n=3 rats). The lower the index, the higher the iron efflux rate (see text). Different lower case letters indicate statistical significant differences between tissues ($p \leq 0.05$). Same letter means no statistical difference.

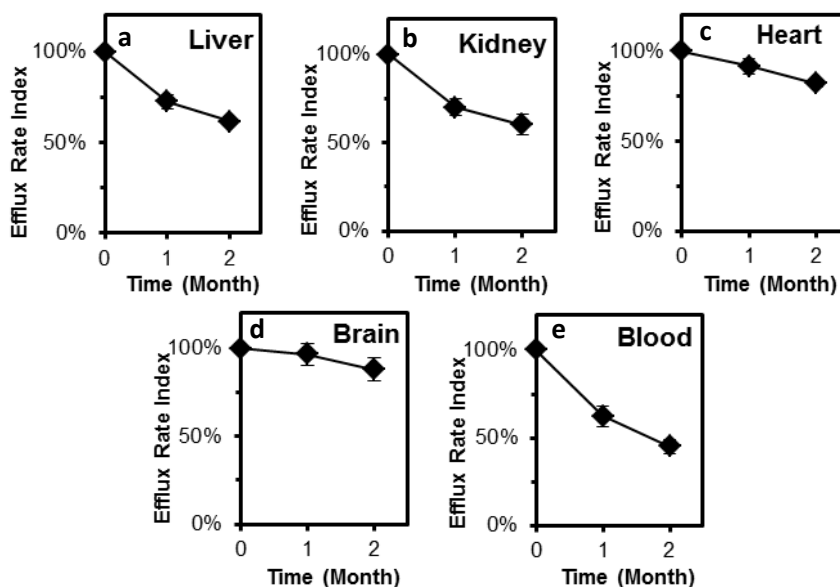


Fig. 7 Changes in Efflux Rate Indices over two months in the *TI* group (n=5). Efflux Rate Indices at month 1 and 2 were normalized to its value at month 0 (Experimental section)

Our understanding of brain iron dynamics is largely based on short-term radiotracer studies. However, due to their instability and radiation safety aspects they are less useful for tracing long-term dietary iron uptake by brain. Long-term feeding of non-decaying stable isotope tracers along with diet, as in our study, allows studying brain iron dynamics over time. Furthermore, the single dose of radiotracers, usually by injection, neglects the homeostatic response of the body and possibly brain to changes in dietary iron supply at the systemic level. This is of significance when studying the role of dietary iron intake in brain iron accumulation.

By feeding iron stable isotopes continuously with diet we were able to assess brain iron balance relative to total brain iron and to consider a possible homeostatic response which was not possible in earlier radiotracer experiments. Because iron has three stable isotopes that can be used as tracers (^{54}Fe , ^{57}Fe and ^{58}Fe), it is possible to use each rat as its own control when studying brain iron dynamics by staggering tracer administration over time (see Fig. 1 and 2). This allows reducing sample size significantly as compared to earlier radiotracer experiments^{23, 24, 30} in which a single tracer was used. Groups of animals in those studies had to be sacrificed at different time points and compared to each other which require naturally larger number of animals to control for inter-individual variations.

Iron balance of an organism/organ depends both on iron influx and efflux rate. Iron accumulates inevitably at the moment that influx rate exceeds efflux with the rate of iron accumulation being determined by their difference. Our understanding of mechanisms of brain iron uptake is still limited despite considerable efforts have been made. Dietary iron was proposed to be taken up by brain either across the blood-brain barrier (BBB, main pathway) or the blood-cerebrospinal fluid barrier (BCB, secondary pathway)^{34, 35}. Many studies suggested that iron uptake across BBB is mainly via transferrin receptor-mediated endocytosis³⁶, while the detection of H-ferritin receptors on BBB suggested an additional pathway^{36, 37}. Expression of iron-related proteins e.g. divalent metal transporter 1, ferroportin, ceruloplasmin and hephaestin were higher in choroid plexus in BCB than virtually all other brain regions³⁸, pointing to alternative mechanisms of brain iron uptake. Our knowledge on iron export is even more limited as it has been studied to a much lower extent. BCB was proposed to be responsible for not only brain iron uptake³⁹ but also iron efflux owing to its structure and functions^{26, 40}. Structurally, tight junctions of BCB are leakier than those of BBB. This is supported by rat studies in which radio-labeled iron was injected into the lateral cerebral ventricle to study iron efflux from cerebrospinal fluid to blood^{27, 40, 41}.

In agreement with earlier radiotracer experiments^{24-27, 40}, our findings support the hypothesis that brain iron uptake is a bi-directional process. Two other studies did not report loss of tracer iron from brain which could be either due to sample size or age of animals^{23, 42}. Observations by Holmes-Hampton et al. (2012)²⁹ point to iron incorporation into brain being biphasic and age-dependent. During early life, iron influx must exceed efflux significantly to cover the high demands for brain development. In the first two years, human brain iron is ca. 50% of the adult brain and approximately doubles within the following decade while it slows down later⁴³.

In good agreement with findings from our earlier study¹⁵ and Bradbury (1997)²⁶, the rank order of the amount of tissue iron uptake was blood > liver > kidney > heart > brain (see Fig. 5). Brain iron turnover was found to be the lowest among the studied organs. The Efflux Rate Index of brain was 0.93 (see Fig. 6), showing that iron turnover rate for brain is slightly higher than for muscle but the lowest of all other studied tissues. This observation is in good agreement with findings by Dallman and Spirito (1977)²⁴ who injected radio-iron into young rats (2-60 days) and monitored brain radioactivity up to 135 days. Their results showed that brain iron radioactivity remained at its peak until the end of the observational period, indicating little/no loss of brain iron during that period. They therefore concluded that brain iron turnover is at an extremely slow rate based on the assumption that mechanisms for brain iron export exist.

In the present study we could estimate that iron that has been transferred from diet to brain is exported at an efflux rate of $8.2 \pm 3.1\%$. However, this figure must be considered the first gross approximation of iron efflux rate of brain in a mammalian organism as only three data points were available per rat for calculation (see Fig. 7). The corresponding half-life of iron tracer in brain, and thus that of dietary iron taken up by brain during adulthood, was 9.4 ± 3.2 months. This can be considered relatively long with regard to the short life time of rats⁴⁴. As iron turnover rate in rat organs cannot be simply extrapolated to humans based on the ratio of their life spans, the data on iron turnover rate in blood in these two species can be of use to extrapolate findings to human brain. The half-life of iron tracer in blood was found to be approximately 83 months in adult men⁴⁵ as compared to ca. 2 months for adult rats (Table 2). At an average human life time of 75 as compared to 3 years in rats, the half-life of iron in human brain can be reasonably estimated to be of the order of decade(s).

Conclusion

In agreement with our earlier study, dietary iron taken up by rat brain amounted to ca. 9% of brain iron after 4 months of tracer feeding. Half of this iron will leave brain within one half-life, i.e. 9 months. Assuming that brain iron uptake and its half-life are constant during adulthood, brain iron of the rats can be estimated to increase by ca. 30% from early adulthood (6-8 months) to end of their life (ca. 36 months).

The present study, for the first time ever, revealed that dietary iron enters adult brain at a significantly higher influx rate than efflux which automatically leads to brain iron accumulation during adulthood. This permits us now to study the effect of dietary iron intake on brain iron accumulation in healthy organisms and in conditions where body iron homeostasis is impaired. Furthermore, the developed methodologies can be used to evaluate treatments to reduce iron burdens in adult brain and thus iron-implicated neurodegeneration.

Acknowledgements

We thank the National University of Singapore for financial support.

Notes and references

^a Department of Chemistry, National University of Singapore, 3 Science Drive 3, Singapore, 117543. walczyk@nus.edu.sg.

^b Department of Nutrition and Food Hygiene, Southern Medical University, Guangzhou 510515, Guangzhou, China, 510515.

^c Department of Biochemistry, National University of Singapore, 8 Medical Drive, Singapore, 117597.

1. R. R. Crichton, D. T. Dexter, R. J. Ward, Brain iron metabolism and its perturbation in neurological diseases. *Monatsh Chem* 2011, *142*. 341-355, DOI: 10.1007/s00706-011-0472-z.

2. S. Altamura, M. U. Muckenthaler, Iron toxicity in diseases of aging: Alzheimer's disease, Parkinson's disease and atherosclerosis. *J Alzheimers Dis* 2009, *16*. 879-895, DOI: 10.3233/Jad-2009-1010.

3. J. P. Kehrer, The Haber-Weiss reaction and mechanisms of toxicity. *Toxicology* 2000, *149*. 43-50, DOI: 10.1016/s0300-483x(00)00231-6.

4. B. Hallgren, P. Sourander, The effect of age on the non-haemin iron in the human brain. *J Neurochem* 1958, *3*. 41-51, DOI: 10.1111/j.1471-4159.1958.tb12607.x.

5. H. R. Massie, V. R. Aiello, V. Banziger, Iron accumulation and lipid peroxidation in aging C57BL/6J Mice. *Exp Gerontol* 1983, *18*. 277-285, DOI: 10.1016/0531-5565(83)90038-4.

6. C. I. Cook, B. P. Yu, Iron accumulation in aging: modulation by dietary restriction. *Mech Ageing Dev* 1998, *102*. 1-13, DOI: 10.1016/S0047-6374(98)00005-0.

7. C. J. Maynard, R. Cappai, I. Volitakis, R. A. Cherny, A. R. White, K. Beyreuther, C. L. Masters, A. I. Bush, Q. X. Li, Overexpression of Alzheimer's disease amyloid-beta opposes the age-dependent elevations of brain copper and iron. *J Biol Chem* 2002, *277*. 44670-44676, DOI: 10.1074/jbc.M204379200.

8. P. A. Hardy, D. Gash, R. Yokel, A. Andersen, Y. Ai, Z. M. Zhang, Correlation of R2 with total iron concentration in the brains of rhesus monkeys. *J Magn Reson Imaging* 2005, *21*. 118-127, DOI: 10.1002/Jmri.20244.

9. P. Hahn, Y. Song, G. S. Ying, X. N. He, J. Beard, J. L. Dunaief, Age-dependent and gender-specific changes in mouse tissue iron by strain. *Exp Gerontol* 2009, *44*. 594-600, DOI: 10.1016/j.exger.2009.06.006.

10. G. Bartzokis, P. H. Lu, K. Tingus, D. G. Peters, C. P. Amar, T. A. Tishler, J. P. Finn, P. Villablanca, L. L. Altshuler, J. Mintz, E. Neely, J. R. Connor, Gender and iron genes may modify associations between brain iron and memory in healthy aging. *Neuropsychopharmacol* 2011, *36*. 1375-1384, DOI: 10.1038/Npp.2011.22.

11. D. B. Kell, Iron behaving badly: inappropriate iron chelation as a major contributor to the aetiology of vascular and other progressive inflammatory and degenerative diseases. *Bmc Med Genomics* 2009, *2*. 2, DOI: 10.1186/1755-8794-2-2.

12. L. Zecca, M. B. H. Youdim, P. Riederer, J. R. Connor, R. R. Crichton, Iron, brain ageing and neurodegenerative disorders. *Nat Rev Neurosci* 2004, *5*. 863-873, DOI: 10.1038/Nrn1537.

13. A. I. Bush, The metal theory of Alzheimer's disease. *J Alzheimers Dis* 2013, *33*. S277-S281, DOI: 10.3233/Jad-2012-129011.

14. H. Kumar, H. W. Lim, S. V. More, B. W. Kim, S. Koppula, I. S. Kim, D. K. Choi, The Role of Free Radicals in the Aging Brain and Parkinson's Disease: Convergence and Parallelism. *Int J Mol Sci* 2012, *13*. 10478-10504, DOI: 10.3390/ijms130810478.

15. J.-H. Chen, S. Shahnavas, N. Singh, W.-Y. Ong, T. Walczyk, Stable iron isotope tracing reveals significant brain iron uptake in adult rats. *Metallomics* 2013, *5*. 167-173, DOI: 10.1039/C2MT20226C.

16. A. Crowe, E. H. Morgan, Effects of chelators on iron uptake and release by the brain in the rat. *Neurochem Res* 1994, *19*. 71-76, DOI: 10.1007/bf00966731.

17. T. Moos, E. H. Morgan, Evidence for low molecular weight, non-transferrin-bound iron in rat brain and cerebrospinal fluid. *J Neurosci Res* 1998, *54*. 486-494, DOI: 10.1002/(Sici)1097-4547(19981115)54:4<486::Aid-Jnr6>3.0.Co;2-I.

18. J. L. Beard, J. A. Wiesinger, N. Li, J. R. Connor, Brain iron uptake in hypotransferrinemic mice: influence of systemic iron status. *J Neurosci Res* 2005, *79*. 254-261, DOI: Doi 10.1002/Jnr.20324.

19. J. Hofstetter, M. A. Suckow, D. L. Hickman, in *The Laboratory Rat*, ed. M. A. Suckow, S. H. Weisbroth, C. L. Franklin. Academic Press, 2th edn., 2006, pp 93-125.

20. T. Walczyk, Iron Isotope Ratio Measurements by Negative Thermal Ionisation Mass Spectrometry Using FeF₄⁻ Molecular Ions. *Int J Mass Spectrom Ion Process* 1997, *161*. 217-227, DOI: 10.1016/S0168-1176(96)04532-6.

21. T. Walczyk, in *Isotopic Analysis*, ed. F. Vanhaecke, P. Degryse. Wiley-VCH Verlag GmbH & Co. KGaA, 2012, pp 435-494.

22. E. J. Underwood, in *Trace elements in human and animal nutrition*, ed. E. J. Underwood. Academic Press, 4th edn., 1977, pp 14-15.

23. E. M. Taylor, E. H. Morgan, Developmental changes in transferrin and iron uptake by the brain in the rat. *Dev Brain Res* 1990, *55*. 35-42, DOI: 10.1016/0165-3806(90)90103-6.

24. P. R. Dallman, R. A. Spirito, Brain iron in rat: extremely slow turnover in normal rats may explain long-lasting effects of early iron deficiency. *J Nutr* 1977, *107*. 1075-1081.

25. W. A. Banks, A. J. Kastin, M. B. Fasold, C. M. Barrera, G. Augereau, Studies of the slow bidirectional transport of iron and transferrin across the blood-brain-barrier. *Brain Res Bull* 1988, *21*. 881-885, DOI: 10.1016/0361-9230(88)90021-4.

26. M. W. B. Bradbury, Transport of iron in the blood-brain-cerebrospinal fluid system. *J Neurochem* 1997, *69*. 443-454, DOI: 10.1046/j.1471-4159.1997.69020443.x.

27. T. Moos, T. R. Nielsen, T. Skjorringe, E. H. Morgan, Iron trafficking inside the brain. *J Neurochem* 2007, *103*. 1730-1740, DOI: 10.1111/j.1471-4159.2007.04976.x.

28. K. M. Erikson, D. J. Pinero, J. R. Connor, J. L. Beard, Regional brain iron, ferritin and transferrin concentrations during iron deficiency and iron repletion in developing rats. *J Nutr* 1997, *127*. 2030-2038.

29. G. P. Holmes-Hampton, M. Chakrabarti, A. L. Cockrell, S. P. McCormick, L. C. Abbott, L. S. Lindahl, P. A. Lindahl, Changing iron content of the mouse brain during development. *Metallomics* 2012, *4*. 761-770, DOI: 10.1039/C2mt20086d.

30. E. M. Taylor, A. Crowe, E. H. Morgan, Transferrin and iron uptake by the brain: effects of altered iron status. *J Neurochem* 1991, *57*. 1584-1592, DOI: 10.1111/j.1471-4159.1991.tb06355.x.

31. A. J. I. Roskams, J. R. Connor, Iron, transferrin, and ferritin in the rat brain during development and aging. *J Neurochem* 1994, *63*. 709-716.

32. S. Takahashi, I. Takahashi, H. Sato, Y. Kubota, S. Yoshida, Y. Muramatsu, Age-related changes in the concentrations of major and trace elements in the brain of rats and mice. *Biol Trace Elem Res* 2001, *80*. 145-158, DOI: 10.1385/Bter:80:2:145.

ARTICLE

- 1
2
3
4
5
6
7
8
9
10
11
12
13
14
15
16
17
18
19
20
21
22
23
24
25
26
27
28
29
30
31
32
33
34
35
36
37
38
39
40
41
42
43
44
45
46
47
48
49
50
51
52
53
54
55
56
57
58
59
60
33. T. Tarohda, M. Yamamoto, R. Amano, Regional distribution of manganese, iron, copper, and zinc in the rat brain during development. *Anal Bioanal Chem* 2004, *380*. 240-246, DOI: 10.1007/s00216-004-2697-8.
34. F. Ueda, K. B. Raja, R. J. Simpson, I. S. Trowbridge, M. W. B. Bradbury, Rate of Fe-59 uptake into brain and cerebrospinal-fluid and the influence thereon of antibodies against the transferrin receptor. *J Neurochem* 1993, *60*. 106-113, DOI: 10.1111/j.1471-4159.1993.tb05828.x.
35. A. Crowe, E. H. Morgan, Iron and transferrin uptake by brain and cerebrospinal fluid in the rat. *Brain Res* 1992, *592*. 8-16, DOI: 10.1016/0006-8993(92)91652-U.
36. R. R. Crichton, in *Iron metabolism: from molecular mechanisms to clinical consequences*, ed. R. R. Crichton. John Wiley & Sons, 3rd edn., 2009, pp 371-372.
37. J. Fisher, K. Devraj, J. Ingram, B. Slagle-Webb, A. B. Madhankumar, X. Liu, M. Klinger, I. A. Simpson, J. R. Connor, Ferritin: a novel mechanism for delivery of iron to the brain and other organs. *Am J Physiol-Cell Ph* 2007, *293*. C641-C649, DOI: 10.1152/ajpcell.00599.2006.
38. T. A. Rouault, D. L. Zhang, S. Y. Jeong, Brain iron homeostasis, the choroid plexus, and localization of iron transport proteins. *Metab Brain Dis* 2009, *24*. 673-684, DOI: 10.1007/s11011-009-9169-y.
39. Y. Ke, Z. M. Qian, Brain iron metabolism: Neurobiology and neurochemistry. *Prog Neurobiol* 2007, *83*. 149-173, DOI: 10.1016/j.pneurobio.2007.07.009.
40. T. Moos, E. H. Morgan, Kinetics and distribution of [Fe-59-I-125]transferrin injected into the ventricular system of the rat. *Brain Res* 1998, *790*. 115-128, DOI: 10.1016/S0006-8993(98)00055-9.
41. C. K. Su, Y. C. Sun, S. F. Tzeng, C. S. Yang, C. Y. Wang, M. H. Yang, In vivo monitoring of the transfer kinetics of trace elements in animal brains with hyphenated inductively coupled plasma mass spectrometry techniques. *Mass Spectrom Rev* 2010, *29*. 392-424, DOI: 10.1002/Mas.20240.
42. T. J. S. Lopes, T. Luganskaja, M. V. Spasic, M. W. Hentze, M. U. Muckenthaler, K. Schumann, J. G. Reich, Systems analysis of iron metabolism: the network of iron pools and fluxes. *Bmc Syst Biol* 2010, *4*. 112, DOI: 10.1186/1752-0509-4-112.
43. FAO, WHO *Iron*; Human vitamin and mineral requirements FAO/WHO: 2001.
44. R. Quinn, Comparing rat's to human's age: How old is my rat in people years? *Nutrition* 2005, *21*. 775-777, DOI: 10.1016/j.nut.2005.04.002.
45. C. A. Finch, Body iron exchange in man. *J Clin Invest* 1959, *38*. 392-396, DOI: 10.1172/Jci103813.